Supporting Information

Surface Optimization to Eliminate Hysteresis for Record Efficiency Planar Perovskite Solar Cells

Dong Yang,[a] Xin Zhou,[c] Ruixia Yang,[b] Zhou Yang,[a] Wei Yu,[b] Xiuli Wang,[b] Can Li,[*b] Shengzhong (Frank) Liu[*a,b] and Robert P. H. Chang[d]

[a]*Key Laboratory of Applied Surface and Colloid Chemistry, National Ministry of Education; Shaanxi Engineering Lab for Advanced Energy Technology, School of Materials Science and Engineering, Shaanxi Normal University, Xi'an 710119, China*

[b]*State Key Laboratory of Catalysis, Dalian National Laboratory for Clean Energy, Dalian Institute of Chemical Physics, Chinese Academy of Sciences, Dalian, 116023, China*

[c]*College of Environmental and Chemical Engineering, Dalian University, Dalian, 116622, China*

[d]*Department of Materials Science and Engineering, Argonne-Northwestern Solar Energy Research (ANSER) Center, Northwestern University, 2145 Sheridan Road, Evanston, Illinois 60208, USA*

Materials

CH_3NH_3I was synthesized and purified according to a reported procedure.[1] Methylamine (24 mL, 33 wt.% in absolute ethanol, Aldrich) and hydroiodic acid (10 mL, 57 wt.% in water, Aldrich) were mixed in 100 mL round-bottom flask at 0 °C for 2 hour with stirring. The precipitate was recovered by removing the solvents at 50 °C using a rotary evaporator. Re-dissolve the product in absolute ethanol, precipitate by adding certain amount of diethyl ether. After extraction filtration, the above steps were repeated for one more time to harvest pure CH_3NH_3I material. Finally, the solid product was dried at 60 °C in a vacuum oven for 24 hour. [6,6]-phenyl-C61-butyric acid methyl ester (PCBM, purity > 99.5%) was purchased from Solarmer Materials Inc. PTAA (Mn = 17.5 kg mol^{-1}, PDI = 1.81) was purchased from EM index. The 1-butyl-3-methylimidazolium tetrafluoroborate ([BMIM]BF_4, $C_8H_{15}N_2BF_4$, purity > 98.5%) and all of the solvents were purchased from Aldrich.

Device fabrication

Glass/FTO was cleaned with acetone, isopropyl alcohol and deionized water successively in ultrasonic bath for 30 min, and then dried by flowing nitrogen gas. The TiO_2 films were sputtered on 33 × 33 mm^2 glass/FTO substrates at room temperature using 400 W for a 3-inch-diameter metallic plate of Ti (99.995%) in an atmosphere of Ar (99.998%) and O_2 (99.998%) by the PVD-75 vacuum system (Kurt J. Lesker, U.S.A), followed by annealing at 500 °C for 30 min. The thickness of the ~45 nm TiO_2 film was determined by a Bruker 150 surface profiler. The IL was dissolved in methanol with different concentration, and spin-coated onto the substrates at 5000 rpm, then annealed at 80 °C for 10 min in glovebox to remove the residual solvent. The perovskite films were deposited onto TiO_2 and m-TiO_2 substrates. Firstly, 150 nm thick $PbCl_2$ film was deposited onto the substrate by evaporation at about 310 °C. The deposition rate was maintained at ca. 1 Å s^{-1} and substrates were kept at room temperature. The $PbCl_2$ samples were transferred into the nitrogen filled glovebox after cooling down to the room temperature, then the $PbCl_2$ samples were placed on a layer of CH_3NH_3I powder, then heated to 150 °C and maintained at the temperature for 20 min to ensure that all $PbCl_2$ was transformed into perovskite. The perovskite samples were transferred into a petri dish and cooled down to the room temperature. The sample was washed with 50 mL isopropanol, and dried by flowing nitrogen, then annealed at 70 °C for 5 min. The thickness of perovskite film was determined to be ~345 nm by the cross-section SEM (Fig. 2b). The PTAA solution was spin-coated onto the perovskite films at 3000 rpm for 30 s by using PTAA/toluene (10 mg/mL) with an addition of 7.5 μL tBP, and 7.5 μL of a solution of 170 mg/mL Li-TFSI in acetonitrile. The thickness of the PTAA film was determined to be ~60 nm by a Bruker 150 surface profiler. Finally, 80 nm of Au electrode was deposited using a thermal evaporator. It is worthwhile to note that the humidity was maintained below 40% for all preparation processes.

Characterization

The *J-V* performance of the PSCs were analyzed by Keithley 2400 source under ambient condition at room temperature, and the illumination intensity was 100 mW cm^{-2} (AM 1.5G Oriel solar simulator). The power output of lamp was calibrated by a NREL-traceable KG5 filtered silicon reference cell. The device area of 0.1134 cm^2 is defined by a metal aperture to avoiding light scattering from the metal electrode into the device during the measurement. The champion device based on m-TiO_2 characterized under delay time changed from 10 ms to 600 ms per step, measurement time from 6 s to 360 s using both forward and reverse scan directions. The EQE was characterized on the QTest Station 2000ADI system (Crowntech. Inc., USA), and the light source is a 300 W xenon lamp. The monochromatic light intensity for EQE was calibrated with a reference silicon photodiode. AFM height images were obtained with a Bruker Metrology Nanoscope III-D atomic force microscope in tapping mode. The work function of samples was measured by KPFM with a Bruker Metrology Nanoscope VIII AFM. Conducting AFM tips (SCM-PIT/PtIr, Bruker, USA) used for this study had a typical spring constant of 2.8 N m^{-1} and a resonance frequency of 75 kHz. Typical scan line frequency was 0.3 Hz and each image contained 512 × 512 pixels. The TRPL spectra were acquired with the time-correlated single photon counting method with an Edinburgh Instruments FLS920 fluorescence spectrometer. The excitation source is a picosecond pulsed diode laser at 406.8 nm with a pulse width of 64.2 ps. All decays were measured with a 4096-channel analyzer. The SEM images were taken by a Quanta 200F microscope (FEI Company) with an accelerating voltage of 20 kV. XRD patterns were measured on a Rigaku diffractometer equipped with a Cu Kα radiation source. XPS measurements were performed in a VG ESCALAB MK2 system with a monochromatized Al Kα under a pressure of 5.0×10^{-7} Pa. The reflection and transmission were acquired by a Varian UV-vis spectrometer, Cary 5000.

Work function of the TiO_2 and m-TiO_2 samples

The work function of the TiO_2 and m-TiO_2 are characterized by KPFM though probing the difference surface potential (SP) between Pt/Ir-coated tip and the samples.[2,3] The different SP is defined as the following Eq. (1):

$$e \times SP = WF_t - WF_s \qquad (1)$$

where e is the elementary charge of electron, WF_s is the work function of sample surface, and WF_t is the work function of Pt/Ir-coated tip. WF_t is calibrated using highly ordered pyrolytic graphite (HOPG) with 4.60 eV of constant work function. Finally, the work function of sample is calculated using Eq. (2):

$$WF_s = 4.6 + e(SP_{HOPG} - SP_s) \qquad (2)$$

The 2 × 2 μm^2 scan area is measured on both HOPG and the samples, and the mean distribution of surface potential is employed as the sample SP. The SP of HOPG, TiO_2 and m-TiO_2 samples are 15 mV, 356 mV and 603 mV, respectively as shown in Fig. S2. Therefore, the work function of the TiO_2 and m-TiO_2 are 4.26 and 4.01 eV, respectively.

Electron mobility of TiO_2 and m-TiO_2

Electron-only devices (FTO/PCBM/ETL/PCBM/Ag) were fabricated to calculate the electron mobility of the samples, including TiO_2 and m-TiO_2, by the SCLC.[4,5] The PCBM solution was prepared in chlorobenzene with a concentration of 20 mg/mL, and spin-coated on FTO surface at 3000 rpm, then annealed at 100 °C for 15 min in a glovebox. The TiO_2 and m-TiO_2 were deposited on PCBM surface. Sequentially, the PCBM films were fabricated on previous samples surface, then annealed at 100 °C for 15 min in a glovebox. The 100 nm-thick Ag were deposited with a shadow mask. The dark *J-V* characteristics of the electron-only devices were measured by a Keithley 2400 source. The mobility is extracted by fitting the *J-V* curves by the Mott-Gurney Eq. (3):

$$J = \frac{9}{8}\varepsilon_0\varepsilon_r\mu_e\frac{(V_{app} - V_r - V_{bi})^2}{L^3} \qquad (3)$$

Where *J* is the current density, ε_0 is the vacuum permittivity, ε_r is the dielectric permittivity of the ETL

materials, L is the thickness of the ETL film, V_{app} is the applied voltage of the device, V_r is the voltage drop due to constant resistance and series resistance across the electrodes,[4] V_{bi} is the built-in voltage due to the different work function of the two electrodes, and μ_e is the electron mobility. The μ_e is calculated from the currents in the square law region. The electron mobility of 3.83×10^{-4} and 1.36×10^{-3} $cm^2 V^{-1} s^{-1}$ for the TiO_2 and m-TiO_2 are calculated from the currents in the square law region, respectively.

Theoretical calculation

All theoretical calculations were performed with the Vienna ab initio simulation package (VASP) and projector augmented wave (PAW) method.[6-9] The wave function was expanded by plane wave with kinetic cutoff of 400 eV. The generalized gradient approximation (GGA) with the spin-polarized Perdew-Burke-Ernzerhof (PBE) function was used for all calculations.[10] The bonding energy is calculated using Eq. (4):

$$E_b = E_{tot} - E_{sur} - E_{mol} \qquad (4)$$

Where E_{tot} is the total energy of the system studied, E_{sur} the energy of a clean surface, and E_{mol} the energy of free IL. The negative bonding energy signifies that the chemisorption structure is stable. The minimum energy E_{tot} for different species adsorbed on the perovskite and the TiO_2 surface were determined by relaxing various initial structures. The binding energies for $[BF_4]^-$ group adsorbed on TiO_2 and on the perovskite surface are -1.24 eV and 1.86 eV, respectively, as shown in Fig S5a and S5b, meaning that $[BF_4]^-$ tend to bond to the TiO_2 surface, rather than to the perovskite layer. Likewise, the binding energies for the adsorbed on TiO_2 and the perovskite surfaces are -1.63 eV and -3.57 eV, respectively as shown in Fig S5c and S5d, implying that the $[BMIM]^+$ is in favor of bonding to the perovskite rather than the TiO_2 surface. The computational results reveal that the IL bonds to both the TiO_2 surface and the perovskite layer due to its strong ionic functional groups.

References

1 N. J. Jeon, J. H. Noh, Y. C. Kim, W. S. Yang, S. Ryu and S. Seok, *Nat. Mater.*, **2014**, *13*, 897.

2 W. Melitz, J. Shen, S. Lee, J. S. Lee, A. C. Kummel, R. Droopad and E. T. Yu, *J. Appl. Phys.*, **2010**, *108*, 023711.

3 L. Zhou, D. Yang, W. Yu, J. Zhang and C. Li, *Org. Electron.*, **2015**, *23*, 110.

4 S. Park, J. H. Heo, C. H. Cheon, H. Kim, S. H. Im and H. J. Son, *J. Mater. Chem. A*, **2015**, *3*, 24215.

5 G. G. Malliaras, J. R. Salem, P. J. Brock and C. Scott, *Phys. Rev. B*, **1998**, *58*, 13411.

6 G. Kesse and J. J. Furthmüller, *Phys. Rev. B*, **1996**, *54*, 11169.

7 G. Kesse and J. Furthmüller, *Comput. Mater. Sci.*, **1996**, *6*, 15.

8 Blöchk, *P. Phys. Rev. B*, **1994**, *50*, 17953.

9 G. Kresse and D. Joubert, *Phys. Rev. B*, **1999**, *59*, 1758.

10 J. P. Predew, K. Burke, and M.Ernzerhof, *Phys. Rev. Lett.*, **1996**, *77*, 3865.

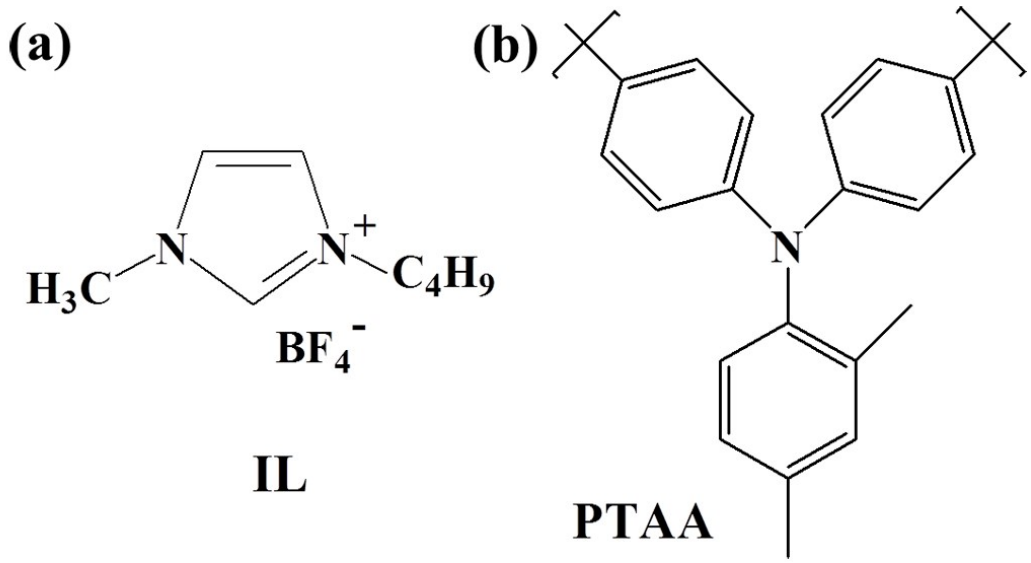

Scheme S1. Chemical structures of (a) 1-butyl-3-methylimidazolium tetrafluoroborate and (b) PTAA molecules.

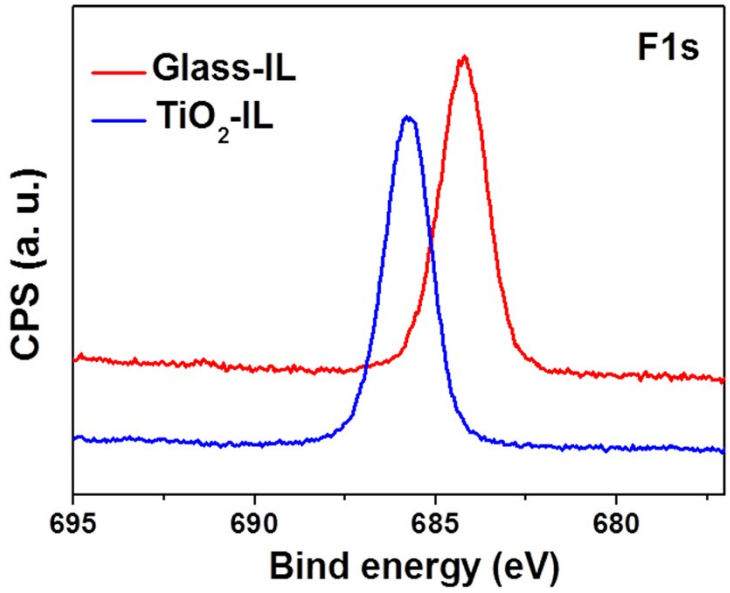

Fig. S1. XPS focus on the F1s peaks for glass-IL and TiO_2-IL samples.

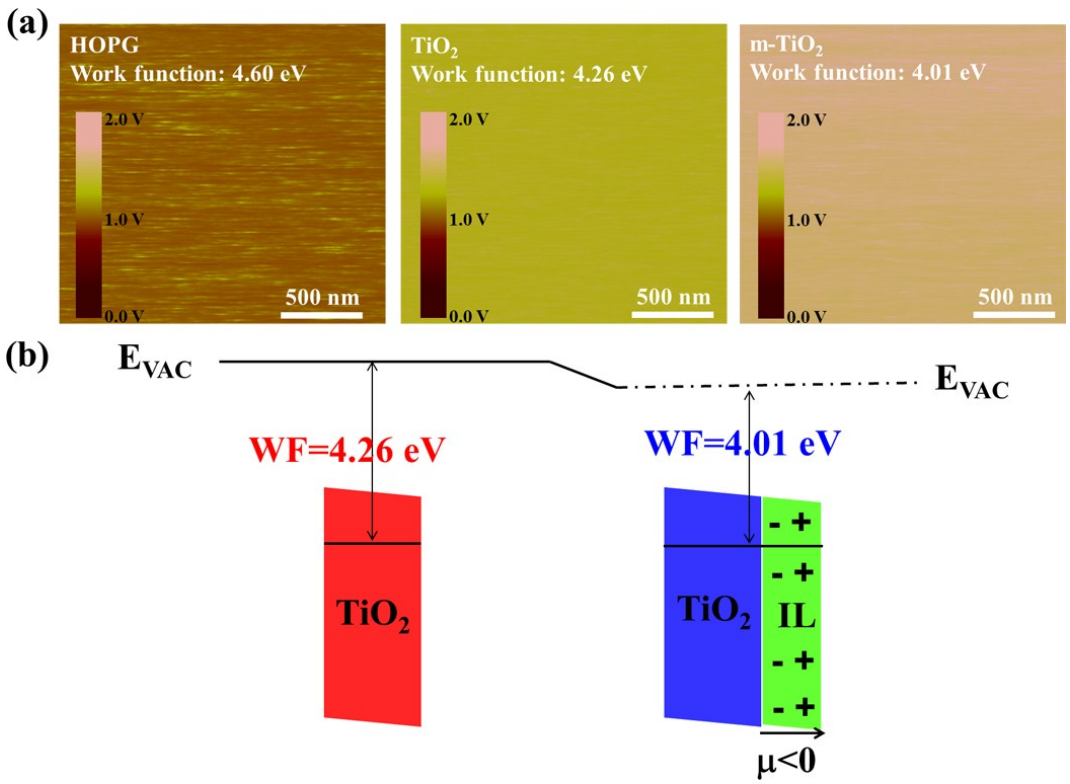

Fig. S2. (a) Surface potential images of HOPG, TiO_2 and m-TiO_2. The surface potential images are original data without further processing. (b) Illustration of vacuum level shift and reduced work function of TiO_2 after the IL modification.

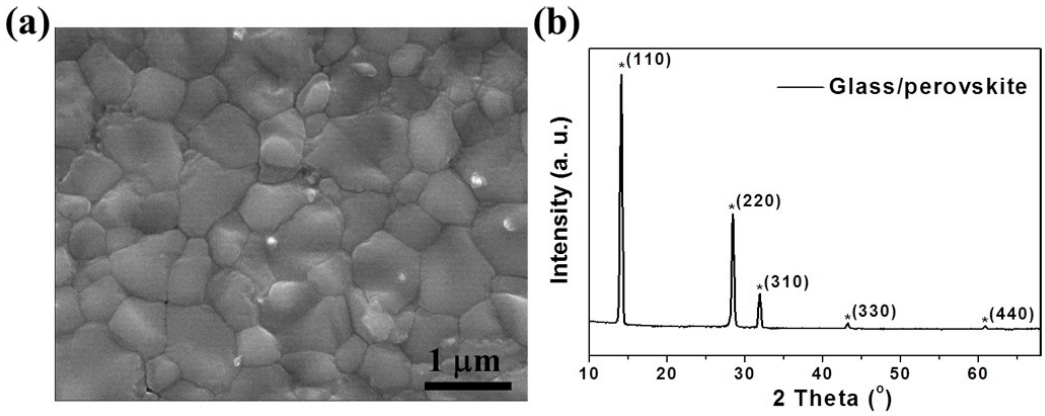

Fig. S3. (a) Top-view SEM image of the perovskite film. (b) XRD spectrum of the perovskite film.

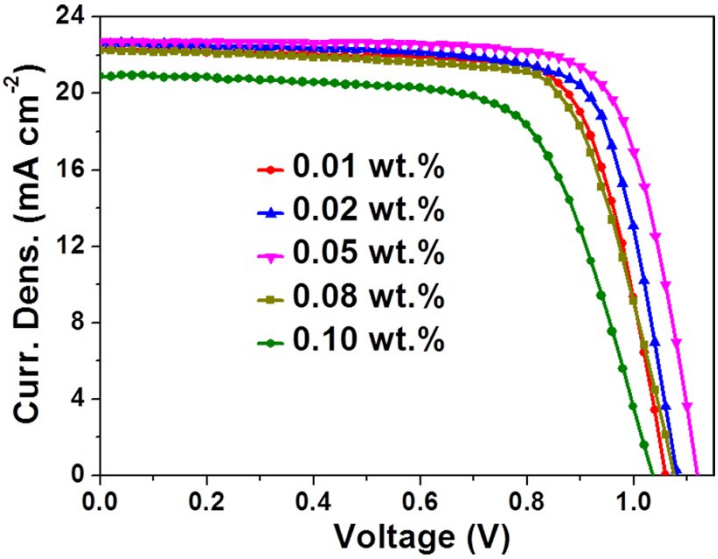

Fig. S4. *J-V* characteristics of the PSCs with different IL concentration to modify TiO_2.

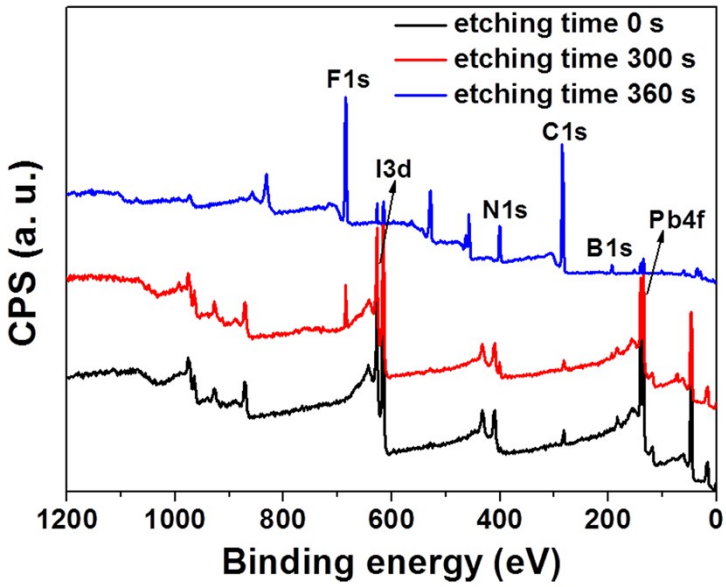

Fig. S5. XPS spectra of the m-TiO_2/$CH_3NH_3PbI_3$ film at the etching time of 0, 300 and 360 seconds.

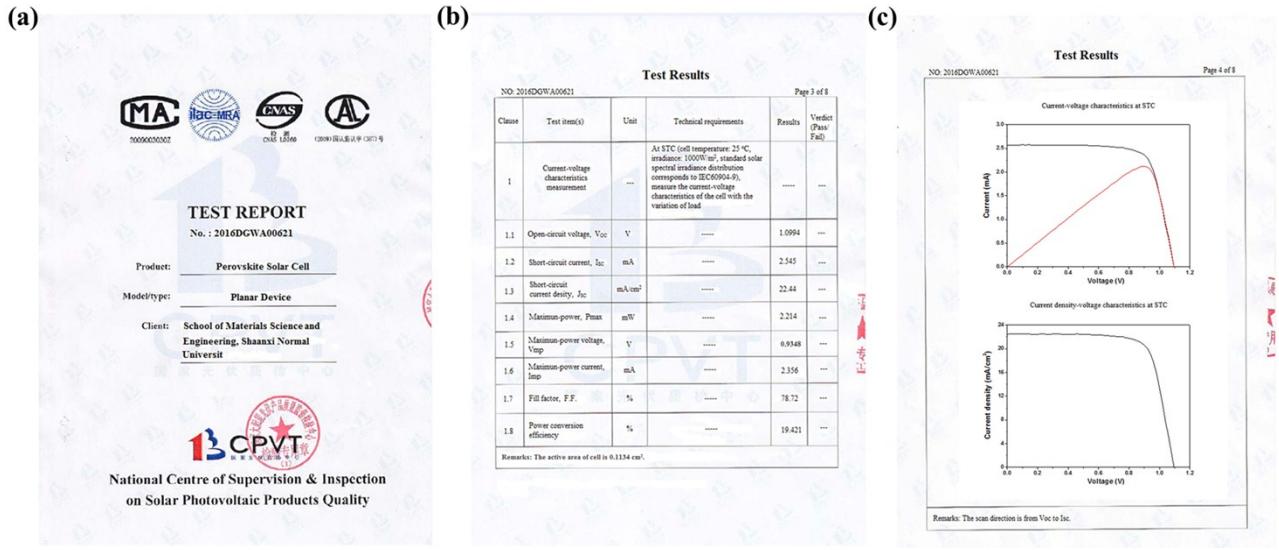

Fig. S6. (a) Cover page of certified report by CPVT on PSC with m-TiO_2 ETL. (b) List of the parameters for device. (c) I-V, power output and *J-V* cures of the PSC based on m-TiO_2.

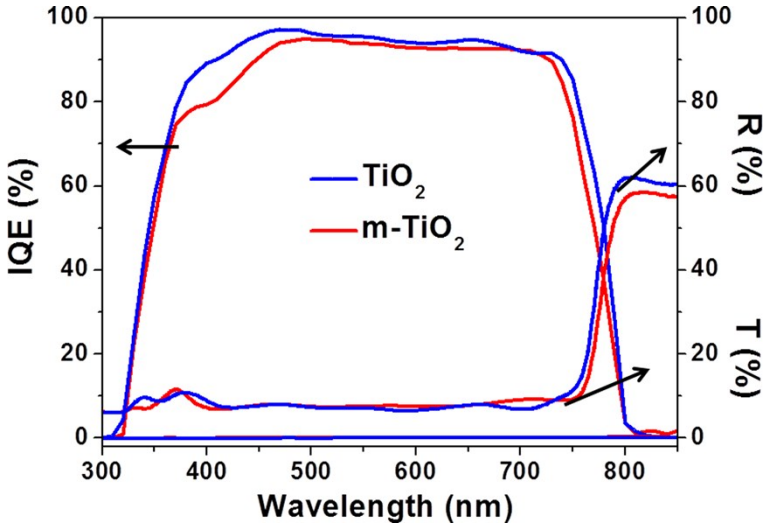

Fig. S7. The IQE, reflection and transmission spectra of PSCs with TiO_2 and m-TiO_2 as ETLs. The IQE is calculated from EQE, reflection and transmission spectra using the Eq. $IQE = \frac{EQE}{1 - R_{loss} - T_{loss}}$, where R_{loss} is reflection loss of device and T_{loss} is transmission loss of device. It is clear that the IQE of m-TiO_2 and TiO_2 for device at ~ 450 nm are 98.7% and 94.9%, respectively.

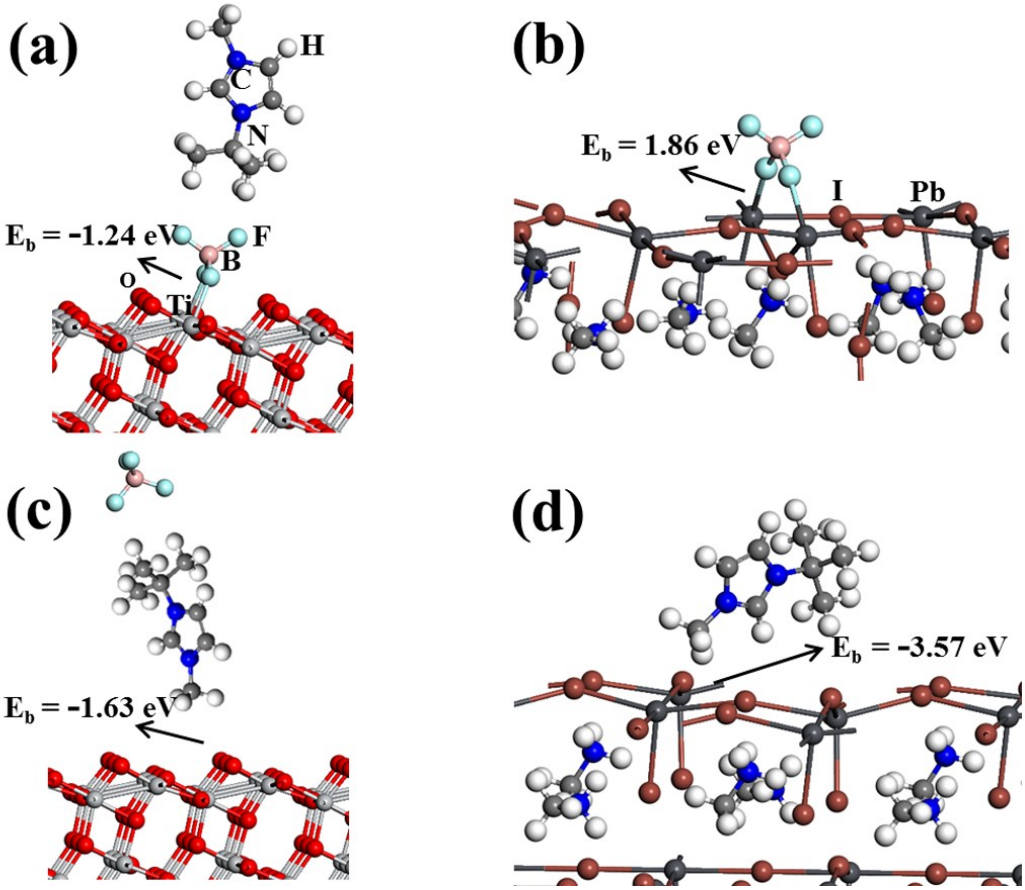

Fig. S8. Minimum energy adsorption geometry of $[BF_4]^-$ on TiO_2 (a) and perovskite (b). Minimum energy adsorption geometry of $[BMIM]^+$ on TiO_2 (c) and perovskite (d). The red, silver, light gray, dark gray, blue, light blue, pink, brown and white balls represent O, Ti, C, Pb, N, F, B, I and H atoms, respectively.

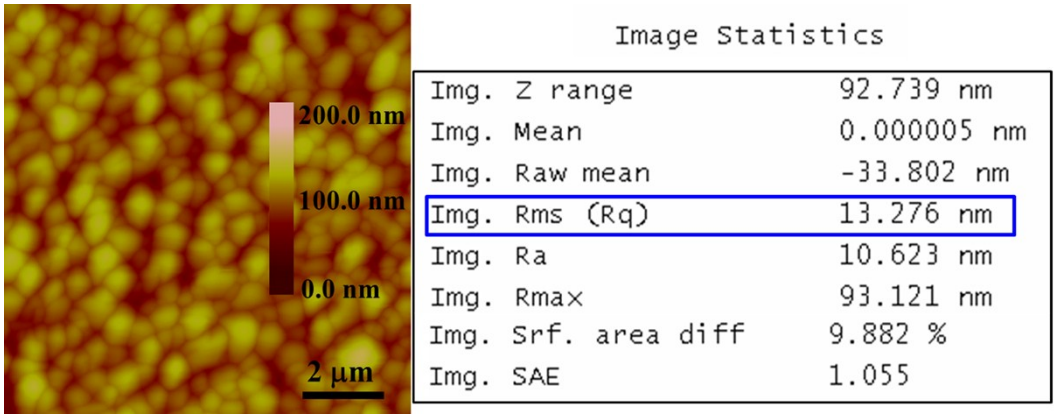

Fig. S9. AFM height image and surface roughness of the perovskite film based on m-TiO_2.

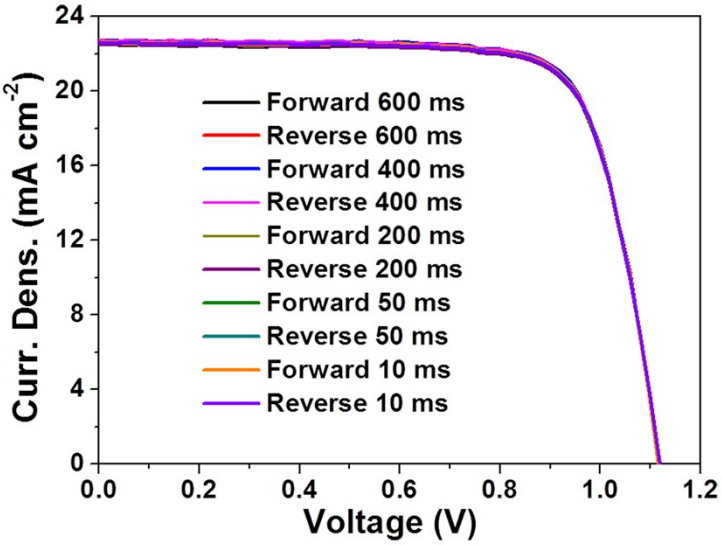

Fig. S10. The *J-V* curves of a PSC based on m-TiO_2 ETL at different scan conditions.

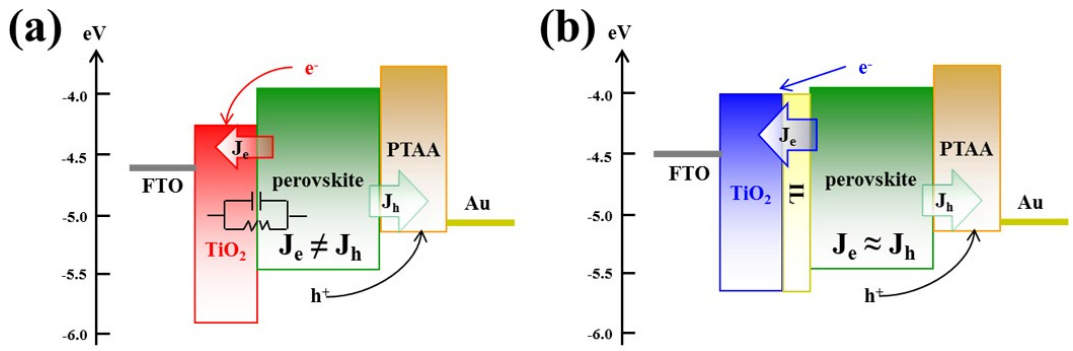

Fig. S11. Carrier transport mechanism of the PSCs employing (a) TiO_2 and (b) m-TiO_2 as ETLs.

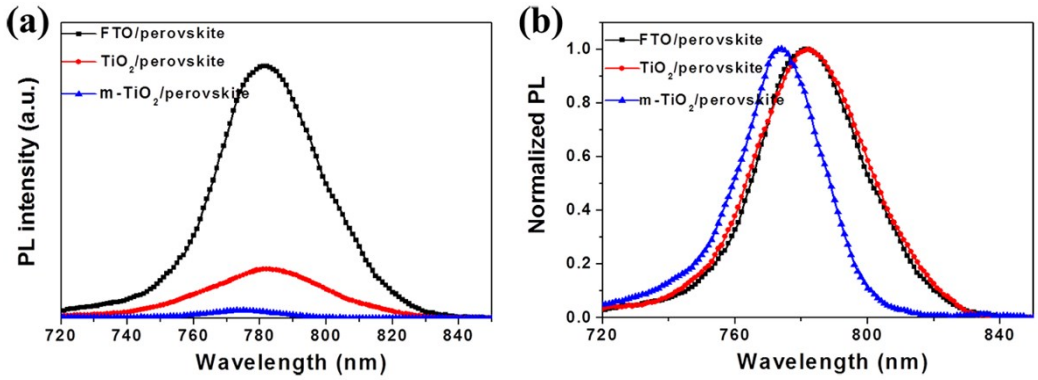

Fig. S12. Steady state PL (a) and normalized PL (b) spectra of FTO/perovskite, TiO_2/perovskite and m-TiO_2/perovskite films.

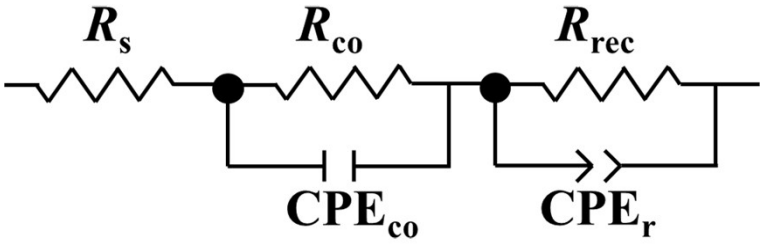

Fig. S13. The equivalent circuit model for PSCs in EIS.

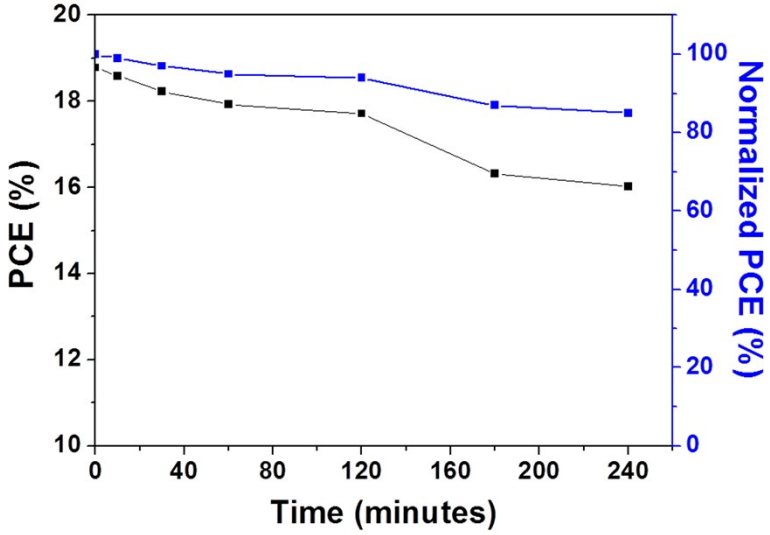

Fig. S14. The PCE stability of a PSC based on m-TiO_2 without any encapsulation under AM 1.5G illumination in ambient conditions.

Table S1. The parameters of PSCs with different IL concentration to modify TiO_2.

IL concentration	J_{sc} (mA cm^{-2})	V_{oc} (V)	FF	PCE (%)	R_s (Ω)	R_{sh} (kΩ)
0.01%	22.25	1.06	0.75	17.69	53	8.76
0.02%	22.66	1.08	0.75	18.36	42	8.97
0.05%	22.75	1.12	0.77	19.62	34	10.62
0.08%	22.25	1.06	0.73	17.22	52	7.46
0.10%	20.91	1.02	0.69	14.72	66	6.17

Table S2. The parameters of PSCs with TiO_2 as ETLs.

Devices	J_{sc} (mA cm^{-2})	V_{oc} (V)	FF	PCE (%)
1	20.55	1.05	0.73	15.75
2	20.32	1.03	0.72	15.07
3	20.75	1.04	0.71	15.32
4	21.05	1.02	0.70	15.03
5	20.05	1.04	0.75	15.64
6	21.38	1.02	0.68	14.83
7	21.04	1.05	0.71	15.69
8	20.56	1.04	0.74	15.82
9	20.67	1.02	0.70	14.76
10	20.18	1.03	0.73	15.17
11	20.77	1.06	0.70	15.41
12	20.37	1.02	0.68	14.13
13	21.04	1.05	0.73	16.13
14	19.77	1.04	0.69	14.19
15	20.06	1.05	0.76	16.01
16	20.19	1.04	0.71	14.91
17	21.37	1.04	0.74	16.45
18	20.11	1.03	0.74	15.33
19	21.27	1.04	0.74	16.37
20	19.40	1.06	0.73	15.01
21	20.54	1.03	0.70	14.81
22	20.66	1.06	0.72	15.77
23	19.83	1.03	0.69	14.09
24	19.69	1.05	0.74	15.30
25	21.27	1.04	0.72	15.93
26	20.05	1.06	0.71	15.09
27	20.58	1.05	0.72	15.56
28	19.94	1.04	0.73	15.14
Average	20.48 ± 0.54	1.04 ± 0.01	0.72 ± 0.02	15.31 ± 0.68

Table S3. The parameters of PSCs based on m-TiO_2.

Devices	J_{sc} (mA cm^{-2})	V_{oc} (V)	FF	PCE (%)
1	22.42	1.06	0.76	18.06
2	22.17	1.06	0.75	17.63
3	22.45	1.08	0.76	18.43
4	22.13	1.08	0.75	17.92
5	22.35	1.08	0.77	18.58
6	22.10	1.07	0.72	17.03
7	22.32	1.08	0.72	17.36
8	21.79	1.08	0.74	17.41
9	22.35	1.06	0.76	18.01
10	21.75	1.08	0.73	17.15
11	21.25	1.08	0.75	17.21
12	22.23	1.08	0.76	18.25
13	22.49	1.08	0.75	18.21
14	21.96	1.09	0.73	17.47
15	22.05	1.08	0.76	18.10
16	22.32	1.08	0.73	17.60
17	22.21	1.10	0.77	18.81
18	22.13	1.08	0.75	17.43
19	22.09	1.08	0.76	18.13
20	22.57	1.10	0.76	18.86
21	22.67	1.10	0.77	19.20
22	22.75	1.12	0.77	19.62
23	22.62	1.08	0.77	18.81
24	22.44	1.08	0.75	18.18
25	22.96	1.09	0.74	18.52
26	22.35	1.09	0.75	18.27
27	22.22	1.08	0.76	18.24
28	22.63	1.07	0.75	18.16
29	22.43	1.08	0.76	18.41
30	22.19	1.08	0.76	18.21
31	22.42	1.08	0.74	17.92
32	22.93	1.10	0.76	19.17
33	22.35	1.08	0.75	18.10
34	21.90	1.07	0.76	17.81
35	22.49	1.08	0.76	18.46
36	22.70	1.08	0.75	18.39
Average	22.31 ± 0.34	1.08 ± 0.01	0.75 ± 0.02	18.14 ± 0.58

Table S4. Parameters of the TRPL spectroscopy based on the FTO/perovskite, TiO_2/perovskite and m-TiO_2/perovskite.

Samples	τ_{ave} (ns)	τ_1 (ns)	τ_2 (ns)	% of τ_1	% of τ_2
FTO/perovskite	25.24	36.06	11.92	28.97	71.03
TiO_2/perovskite	11.46	19.34	1.63	9.50	90.50
m-TiO_2/perovskite	7.09	13.15	1.02	7.21	92.79

Table S5. EIS parameters for the PSCs based on TiO_2 and m-TiO_2.

Substrates	R_s (Ω)	R_{co} (Ω)	R_{rec} (Ω)	CPE_{co}-T (F)	CPE_{co}-P	CPE_r-T (F)	CPE_r-P
TiO_2	38.8	82.6	229.4	3.6×10^{-9}	1.17	2.5×10^{-8}	1.04
m-TiO_2	36.5	64.7	468.5	6.3×10^{-9}	1.14	1.79×10^{-8}	1.05